Cytoplasmic lipid droplets are translocated into the lumen of the *Chlamydia trachomatis* parasitophorous vacuole

Jordan L. Cocchiaro[†], Yadunanda Kumar[†], Elizabeth R. Fischer[‡], Ted Hackstadt[§], and Raphael H. Valdivia[†¶]

[†]Center for Microbial Pathogenesis, Department of Molecular Genetics and Microbiology, Duke University Medical Center, Durham, NC 27710; and [‡]RTB/Research Technologies Section, Microscopy Unit, and [§]Host–Parasite Interactions Section, Rocky Mountain Laboratories, National Institutes of Health, Hamilton, MT 59840

Edited by Stanley Falkow, Stanford University, Stanford, CA, and approved April 7, 2008 (received for review December 26, 2007)

The acquisition of host-derived lipids is essential for the pathogenesis of the obligate intracellular bacteria *Chlamydia trachomatis*. Current models of chlamydial lipid acquisition center on the fusion of Golgi-derived exocytic vesicles and endosomal multivesicular bodies with the bacteria-containing parasitophorous vacuole ("inclusion"). In this study, we describe a mechanism of lipid acquisition and organelle subversion by *C. trachomatis*. We show by live cell fluorescence microscopy and electron microscopy that lipid droplets (LDs), neutral lipid storage organelles, are translocated from the host cytoplasm into the inclusion lumen. LDs dock at the surface of the inclusion, penetrate the inclusion membrane and intimately associate with reticulate Bodies, the replicative form of *Chlamydia*. The inclusion membrane protein IncA, but not other inclusion membrane proteins, cofractionated with LDs and accumulated in the inclusion lumen. Therefore, we postulate that the translocation of LDs may occur at IncA-enriched subdomains of the inclusion membrane. Finally, the chlamydial protein Lda3 may participate in the cooption of these organelles by linking cytoplasmic LDs to inclusion membranes and promoting the removal of the LD protective coat protein, adipocyte differentiation related protein (ADRP). The wholesale transport of LDs into the lumen of a parasitophorous vacuole represents a unique mechanism of organelle sequestration and subversion by a bacterial pathogen.

ADRP | inclusion | Lda3 | organelle translocation

The obligate intracellular pathogen *Chlamydia trachomatis* causes a wide range of ailments including trachoma, conjunctivitis, epididymitis and pelvic inflammatory disease, with different serovars and biovars displaying selective tropism for ocular and genital epithelia (1). *Chlamydia* has a biphasic life cycle with an environmentally stable and inert form, the Elementary Body (EB) and a vegetative metabolically active form, the reticulate body (RB) (2). RBs replicate within a membrane bound parasitophorous vacuole, termed an "inclusion," that is largely inaccessible to endocytic traffic or secretory glycoproteins (3).

Chlamydia efficiently acquires host-derived membrane lipids such as glycerophospholipids (4), sphingolipids (5), and cholesterol (6) by selectively rerouting Golgi-derived exocytic vesicles (7) and multivesicular bodies (MVB) (8). However, membrane lipids are also transported to the inclusion via nonvesicle mediated pathways. For example, the transport of cholesterol and sphingolipids to the inclusion is only partially inhibited by Brefeldin A, an inhibitor of vesicular transport in the Golgi apparatus (6, 7), and acquisition of eukaryotic glycerophospholipids by RBs is entirely Brefeldin A-insensitive (4). Bacterial import of host-derived phospholipids requires deacylation by the host cell's Ca^{2+}-dependent cytosolic Phospholipase A2 (cPLA2) to release lysophospholipid (lyso-PL) and a free fatty acid (9). Lyso-PL is then reacylated by a bacterial branched-chain fatty acid before membrane incorporation (4). Because the inclusion membrane restricts the diffusion of cytoplasmic components >520 Da (10), it is unlikely that protein lipid carriers can freely diffuse into the inclusion lumen. Unfortunately, because there are no genetic tools to manipulate *Chlamydiae*, little is known about the bacterial factors that mediate lipid transport across the inclusion membrane. A diverse family of *Chlamydia* inclusion membrane proteins (Inc) (11) have been postulated to participate in rerouting lipid traffic to the inclusion (3). In addition, *C. trachomatis* secretes proteins (Lda proteins) (12) that bind to cytoplasmic lipid droplets (LDs), neutral lipid storage organelles (13).

LDs consist of a core of neutral lipids surrounded by a phospholipid monolayer (13). Current thought is that LDs originate from the endoplasmic reticulum (ER) where esterified fatty acids and cholesterol accumulate between the membrane bilayer leaflets and eventually bud off into the cytoplasm (13). LDs also have a large number of associated proteins that impact function. The Perilipin-Adipophilin/ADRP-TIP47 (PAT) family of LD-associated proteins regulate the basal rate of lipolysis by forming a protective "coat" that limits the access of lipases to the LD core (14). Overexpression of perilipin or ADRP increases triacylglyceride levels and the formation of LDs (15). In adipocytes, extracellular signals lead to the redistribution of PAT proteins and the subsequent recruitment of neutral-lipid lipases (14) to generate fatty acids for *de novo* membrane biosynthesis and β-oxidation by peroxisomes and mitochondria (16). Mammalian LDs are also enriched in proteins with known functions in vesicular transport, cell signaling (17, 18), and enzymes that generate proinflammatory lipids (19). The presence of these proteins in LDs raises the intriguing possibility that these organelles may influence signaling and inflammatory processes in addition to regulating lipid homeostasis.

Because *Chlamydia* could modulate a range of host cellular functions by targeting LDs, we characterized the interaction of LDs with the inclusion. Here, we document the unexpected finding that cytoplasmic LDs are translocated across the inclusion membrane into the lumen of the parasitophorous vacuole. Furthermore, we provide evidence that a chlamydial protein may be involved in the capture and reprogramming of cytoplasmic LDs by removing a key modulator of its lipid storage functions.

Results

***The Chlamydia* Inclusion Is Enveloped in Neutral Lipid-Rich Reticular Structures and Lipid Droplets (LDs).** The fluorescent neutral lipid dye BODIPY 493/503 labels reticular structures and scattered

Author contributions: J.L.C., Y.K., T.H., and R.H.V. designed research; J.L.C., Y.K., E.R.F., T.H., and R.H.V. performed research; E.R.F. and T.H. contributed new reagents/analytic tools; J.L.C., Y.K., T.H., and R.H.V. analyzed data; and J.L.C. and R.H.V. wrote the paper.

The authors declare no conflict of interest.

This article is a PNAS Direct Submission.

¶To whom correspondence should be addressed. E-mail: valdi001@mc.duke.edu.

This article contains supporting information online at www.pnas.org/cgi/content/full/0712241105/DCSupplemental.

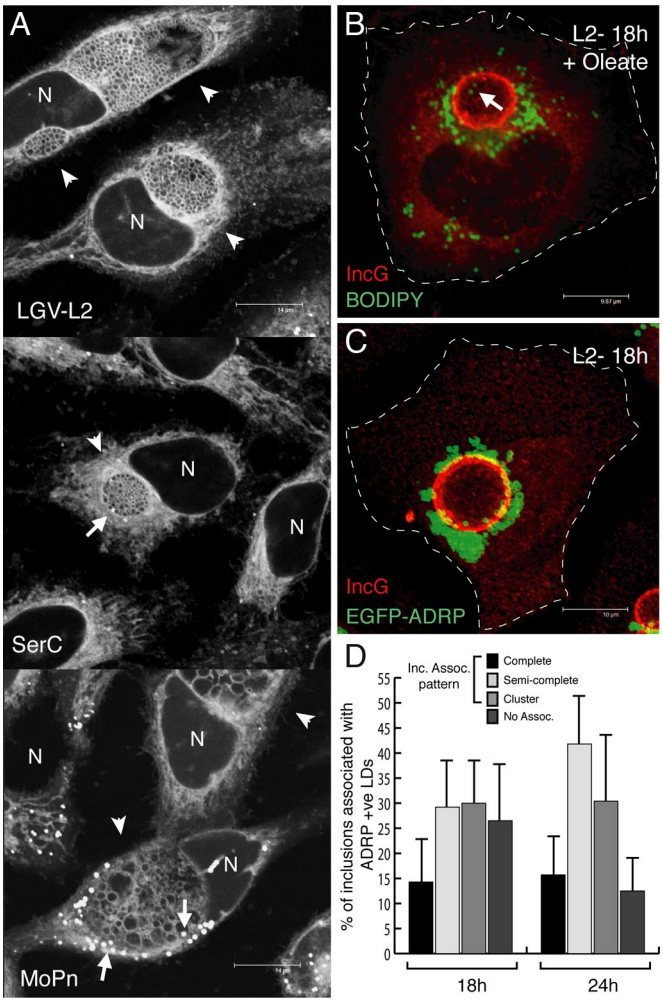

Fig. 1. Neutral lipid-rich reticular structures and Lipid Droplets (LDs) accumulate at the periphery of the *C. trachomatis* inclusion. (*A*) The neutral lipid dye BODIPY 493/503 labels *C. trachomatis* inclusions. HeLa cells were infected with *C. trachomatis* serovars L2, C and the mouse pneumonitis strain, MoPn, for 24–32 h and stained with the neutral lipid dye BODIPY 493/503. Note extensive BODIPY-positive reticular structures enveloping inclusions (arrowheads) and scattered bright lipid droplets (arrows). (*B–D*) LDs associate with the inclusion periphery. The formation of LDs was enhanced by addition of 100 μM oleic acid (*B*) or overexpression of EGFP-ADRP (*C*) and the degree of LD association with inclusions was assessed at various stages in the infectious cycle (*D*) (see Fig. S1 for details). Inclusion membranes were detected with anti-IncG antibodies. (*B–C*) Shown are fixed average projections of confocal stacks. Note the accumulation of distinct mature LDs at the periphery of the inclusions. (*D*) Data represent the mean ± SD from three independent experiments. N, nuclei

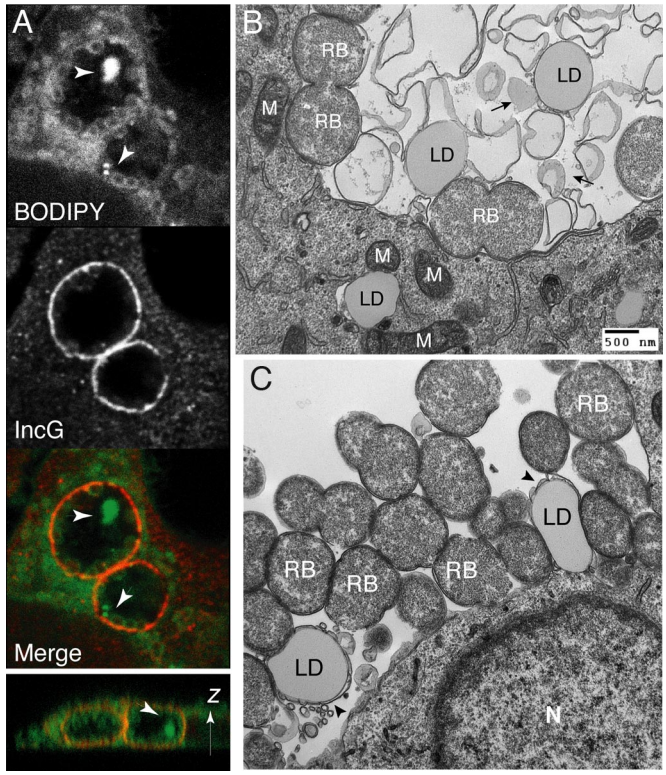

Fig. 2. Intact LDs are present in the chlamydial inclusion lumen. (*A*) Neutral lipid-rich droplets are found within inclusions. Nonlipid loaded HeLa cells were infected with L2 for 20 h and the interaction between inclusions and neutral lipid-rich droplets assessed as in Fig. 1*B*. Note the presence of distinct droplets (arrowheads) within IncG-positive membranes in *xy* (*Top*) and *zy* (*Lower*) laser scanning confocal sections. (*B* and *C*) Ultrastructural analysis of inclusions reveals intact LDs in the inclusion lumen. HeLa cells were infected with L2 for 18 h, fixed in the presence of malachite green to preserve lipid structures, and processed for electron microscopy. LDs, internal membrane structures, and LD-like structures (black arrows) accumulated inside the inclusion. Note membrane blebs associated with intrainclusion LDs (arrowheads) and contacts between LDs, RBs, and the inclusion membrane (*C*). N, HeLa nuclei; M, mitochondria.

"classical" LDs in HeLa cells grown in standard tissue culture media. In contrast, when HeLa cells are infected with *C. trachomatis* genital serovars, ocular serovars, or the mouse pneumonitis strain MoPn, the periphery and lumen of inclusions are prominently labeled with BODIPY (Fig. 1*A*). Because HeLa cells do not accumulate the large LDs commonly observed in adipocytes and lipid-loaded cells, we enhanced LD formation by adding 100 μM oleic acid to growth media or overexpressing ADRP and assessed LD interaction with the inclusion. Neither of these treatments adversely affected chlamydial replication (data not shown). Both BODIPY- and EGFP-ADRP positive LDs preferentially associated with the periphery of inclusions as early as 18 h after infection ($P < 0.01$, Student's t test, for combined association vs. nonassociation phenotypes at 18 and 24 h) [Fig. 1 *B–D* and supporting information (SI) Fig. S1]. Based on these results, we postulate that the BODIPY-positive reticular structures enveloping the inclusion constitute sites of neutral lipid biosynthesis and, by extension, LD assembly.

LDs Are Translocated into the Lumen of the *Chlamydia* Inclusion. We also observed BODIPY-positive droplets in close association with inclusion membranes and within the inclusion lumen, especially when LD formation was enhanced by oleic acid treatment (e.g., Fig. 1 *A* and *B*, arrows). To confirm that these neutral lipid-rich droplets were within the inclusion lumen, even in the absence of lipid-loading, we costained the inclusion membrane with antibodies against Inclusion membrane protein G (IncG) and assessed the subcellular localization of BODIPY-positive structures by laser scanning confocal microscopy (LSCM). Although the detergent permeabilization led to a reduction in BODIPY staining from reticular structures and RBs, droplet-like material was readily apparent in the inclusion lumen (Fig. 2*A*). Intrainclusion and inclusion membrane-associated BODIPY-positive droplets of various sizes were present in >70% of inclusions (data not shown).

Because we could not distinguish between bona fide LDs and aggregates of neutral lipid-rich membranes by light microscopy, we performed ultrastructural analysis of infected cells to deter-

mine the nature of these structures. LDs are disrupted by fixatives and organic solvents commonly used for electron microscopy applications. Therefore, we specifically preserved lipid-rich structures by fixing infected cells in the presence of malachite green (20) before processing the samples for transmission electron microscopy (TEM). This fixation methodology revealed previously unappreciated structural complexity inside the inclusion lumen, including intact LDs (Fig. 2 *B* and *C*). Intrainclusion LDs displayed all of the features of cytoplasmic LDs, including a thin phospholipid monolayer and weak staining of the lipid core. Intrainclusion LDs were often associated with the inclusion membranes and bacterial outer membranes (Fig. 2*B*). LDs entering the inclusion were occasionally surrounded by membrane blebs and vesicles (Fig. 2*C*), presumably originating from the inclusion membrane. In addition, the inclusion lumen displayed a significant amount of debris including electron dense material and membranous structures of unknown origin (Fig. 2*B*). Overall, our LSCM and TEM observations established the presence of LDs in the inclusion lumen and led us to hypothesize that these organelles are translocated from the cytoplasm of the infected cell.

Inclusion Membrane Protein IncA Cofractionates with LDs and Accumulates in the Inclusion Lumen. TEM analysis revealed LDs at different stages of translocation into the inclusion lumen, with LDs occasionally remaining associated with inclusion membranes (Fig. 3*A*). Therefore, we predicted that a portion of inclusion membranes would cofractionate with LDs. To test this, we isolated LDs from infected and uninfected HeLa cells grown in 100 μM oleic acid for 12 h to obtain enough material for reliable biochemical analysis. Because Rab and 14–3-3 proteins have been reported to bind to inclusion membranes (21, 22) and copurify with LDs (18), we tested whether these proteins displayed differential association with LDs during infection. Rab1 and Rab11 cofractionated with LDs, but this association was independent of *Chlamydia* infection (Fig. 3*B*). In contrast, we were unable to detect 14–3-3β in LDs. Next, we assessed a variety of Inc proteins including IncG, IncA, CT223, CT229, and the nonclassical Inc protein, Cap1 for presence in LDs. Interestingly, only IncA significantly associated with purified LDs (Fig. 3*B*), suggesting that inclusion membranes do not cofractionate in bulk with translocating LDs.

The relative enrichment of IncA with LDs suggested that IncA may mark sites on the inclusion membrane permissive for LD translocation. As such, we predicted that IncA-positive membranes should accumulate in the inclusion lumen. To test this, HeLa cells were infected for 18 and 24 h, processed for immunofluorescence with anti-IncA and anti-IncG antibodies, and analyzed by LSCM. IncA localized to the inclusion membrane as described in ref. 23, to distinct intrainclusion aggregates (Fig. 3 *C* and *D*). These aggregates did not colocalize with chlamydial LPS (data not shown), suggesting that IncA in the lumen was not associated with bacterial membranes. Because these intrainclusion structures were recognized by two different sources of anti-IncA polyclonal antibodies (Fig. 3*C* and not shown) and an anti-IncA monoclonal antibody (Fig. 3*D*), it is unlikely that these structures are artifacts of immunostaining procedures. In contrast, IncG was primarily restricted to the inclusion membrane (Fig. 3 *C* and *D*). The association of IncA-positive membranes and LDs is likely transitory as intrainclusion BODIPY-positive droplets only show partial colocalization with lumenal IncA by LSCM (Fig. 3*E*). Based on these observations, we propose that LD-associated IncA represents segments of inclusion membrane that invaginate into the lumen and remain transiently associated with intrainclusion LDs.

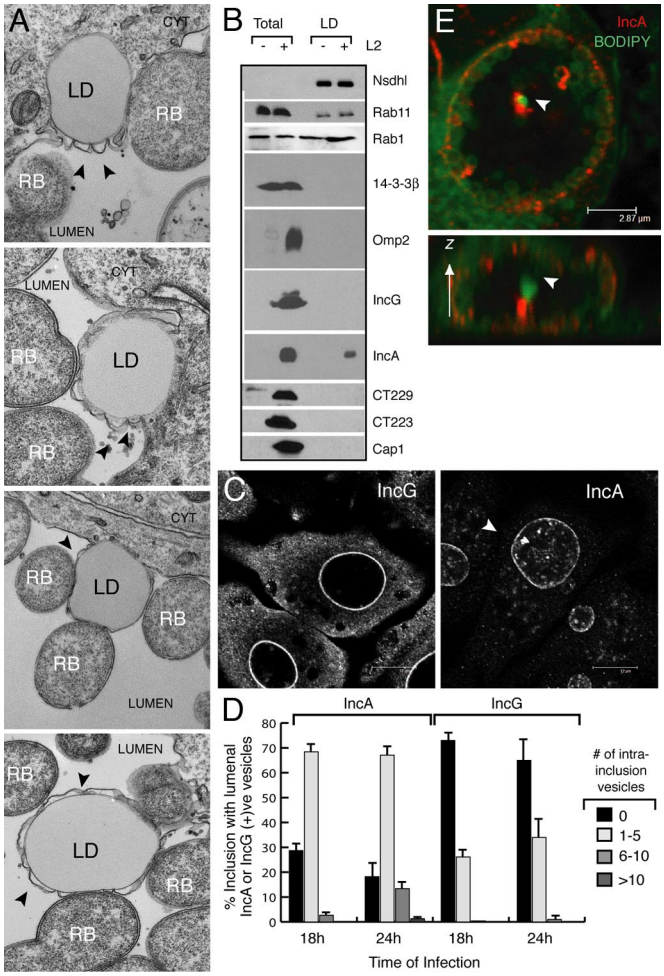

Fig. 3. The inclusion membrane protein IncA copurifies with LDs and accumulates in the inclusion lumen. (*A*) Translocation of LDs across the inclusion membrane. Representative electron micrographs of L2 inclusions show LDs at various stages of crossing the inclusion membrane. Note membranes and blebs (arrowheads) associated with translocating LDs. CYT, cytoplasm. (*B*) IncA cofractionates with LDs. HeLa cells were infected with L2 for 40 h and treated with 100 μM OA 12–14 h before purification of LDs by density gradient ultracentrifugation. The fractionation of a host LD protein (Nsdhl), chlamydial outer membrane protein (Omp2), host proteins associated with the inclusion membrane (Rab11 and 14–3-3β), and Inc proteins (CT223, CT229, IncA, IncG and Cap1) were assessed by immunoblots. Note cofractionation of IncA with purified LDs and lack of other Inc proteins. (*C* and *D*) IncA-positive structures accumulate in the inclusion lumen. HeLa cells were infected with L2 for 18 and 24 h and immunostained with polyclonal anti-IncG or anti-IncA antibodies. Note the accumulation of IncA-positive material in the inclusion lumens (*C*). The frequency of IncA and IncG-positive intrainclusion vesicles (*D*) was determined by LSCM as in *C*, except that an anti-IncA mAb was used. Inclusions (150–300 per time point per experiment) were binned in categories according to the number of vesicles per inclusion. Data represent the mean ± SD of three independent experiments. The number of inclusions with intralumenal IncA-positive vesicles was significantly higher than IncG-positive ($P < 0.001$). (*E*) Partial colocalization of IncA-positive membranes with intrainclusion LDs. HeLa cells were infected with L2 and processed as in Fig. 2*A* with anti-IncA antibodies and BODIPY.

Lda3 Binds to the Inclusion Membrane, and Lda3-Tagged LDs Are Translocated into the Inclusion Lumen. We hypothesized that the chlamydial Lda proteins (12) might participate in the capture, translocation and eventual processing of LDs in the inclusion lumen. Lda3, in particular, is an attractive candidate as a mediator of LD recognition at the inclusion surface. Lda3 is conserved among *Chlamydiae*, anti-Lda3 antibodies label retic-

MICROBIOLOGY

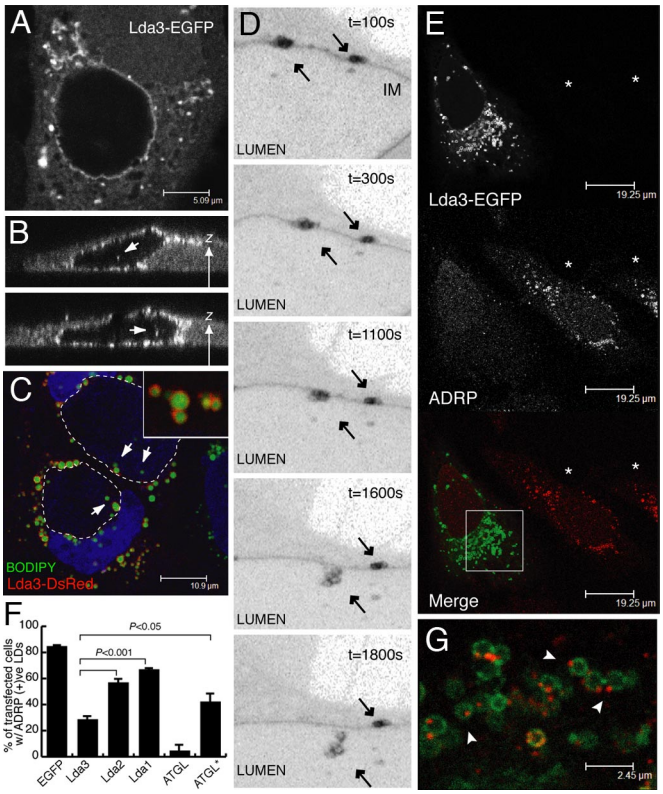

Fig. 4. Exogenously expressed Lda3 binds to LDs and inclusion membranes and induces loss of ADRP. (*A–C*) Lda3-EGFP localizes to inclusion membranes and LDs. HeLa cells expressing Lda3-EGFP were infected with L2 for 20 h (*A* and *B*) and imaged by LSCM. Lda3-EGFP localized prominently to LDs at the periphery of the inclusion and inclusion membranes (*A*). Intrainclusion Lda3-positive material (arrows) was apparent in *xz* confocal sections (*B*). These intrainclusion structures are likely LDs as Lda3-DsRed positive structures in OA-treated cells also stain with BODIPY. (*Inset*) Magnification of Lda3-positive LDs (*C*). (*D*) Live cell analysis of LD translocation into the inclusion lumen. HeLa cells expressing Lda3-EGFP were infected with L2 for 30 h and imaged for 30 min. Representative frames show Lda3-EGFP tagged LDs (arrows) docked at the inclusion lumen in the process of translocation (see Movie S2). (*E–G*) Lda3-EGFP expressing cells display reduced levels of ADRP. HeLa cells were transiently transfected with Lda3-EGFP, treated with 100 μM OA for 12 h, and fixed. ADRP on LDs was detected by indirect immunofluorescence. Prominent localization of ADRP to LDs was only observed in untransfected cells (*). (*E*). The loss of ADRP from LDs was most pronounced in Lda3 compared with Lda1, $Lda2_{LD}$, and a catalytically inactive ATGL (ATGL*). Overexpression of wild-type ATGL led to a loss ADRP. Data represent the mean ± SD of triplicates (*F*). Close up of Lda3-EGFP (green) positive LDs revealed a displacement of endogenous ADRP (red) to distinct puncta on the surface of LDs (arrowheads) (*G*). IM, inclusion membrane.

ular structures closely associated with the cytoplasmic face of the inclusion membrane, and Lda3-EGFP expressed in mammalian cells localizes to LDs (12). To begin to evaluate the role of Lda3 in coopting LDs, we followed the fate of ectopically expressed Lda3 in *Chlamydia*-infected cells. HeLa cells were transfected with an Lda3-EGFP expression vector, infected for 18 and 32 h, and imaged by LSCM. Surprisingly, Lda3-EGFP prominently labeled the inclusion membrane in addition to LDs, especially at later stages in infection (Fig. 4*A*). These results indicated that Lda3 could potentially provide a physical link between LDs and the inclusion. We also detected Lda3-EGFP within the inclusion lumen (Fig. 4*B*), suggesting that cytoplasmic Lda3 had translocated across the inclusion membrane. When Lda3-DsRed was expressed in oleic acid-treated cells, LDs that were positive for both Lda3-DsRed and BODIPY were observed in the cytoplasm and inclusion lumen, suggesting that the intrainclusion Lda3-positive structures are likely LDs (Fig. 4*C*).

We took advantage of the dual tropism of Lda3-EGFP to monitor the interaction of LDs with the inclusion in real time. Selected frames from a time-lapse series show the translocation of Lda3-tagged LDs docked on the inclusion membrane into the lumen (Fig. 4*D* and Movie S1). Lda3-labeled LDs were present close to the inclusion and in contact with the inclusion membrane. Furthermore, time-lapse microscopy revealed that the association of Lda3-tagged LDs with inclusion membranes is dynamic, with docking and partial penetration stages that are reversible, especially in early- to mid-cycle inclusions (<24 h) (Movie S2). However, LDs bound to the inclusion membrane in mature inclusions (>30 h) either ceased to move or displayed restricted movement on the plane of the membrane (Movie S1).

LDs are heterogenous organelles with distinct protein compositions that may reflect different cellular functions (24). To determine whether Lda3 labels all LDs, we expressed EGFP and Lda3-EGFP in lipid-loaded HeLa cells and monitored the colocalization of Lda3 with ADRP, a pan-LD marker. Untransfected and EGFP-expressing cells displayed abundant ADRP-positive LDs. In contrast, Lda3-EGFP positive transfectants had a marked decrease in overall ADRP staining (Fig. 4*E*). The loss of ADRP was more prominent in Lda3 transfected cells compared with Lda1, the LD-binding domain of Lda2 ($Lda2_{LD}$), and a catalytic mutant of the LD-associated lipase ATGL (25) (Fig. 4*F*). Closer examination of LDs in transfected cells revealed that any remaining endogenous ADRP was restricted to distinct puncta on the surface of Lda3-EGFP positive LDs (Fig. 4*G*).

Overall, these results demonstrate that exogenously expressed Lda3 remains associated with LDs during the initial translocation into the inclusion lumen and that the association of ADRP with LDs decreases upon Lda3 overexpression.

Discussion

Chlamydia places a large metabolic burden on its host cell, as revealed by increased rates of mitochondrial respiration (26) and long-chain fatty acid (LCFA) uptake (27). Because LDs are a rich source of esterified LCFA and LCFAs play a central role as high-energy substrates and precursors in PL biosynthesis, it is perhaps not surprising that *C. trachomatis* would have evolved mechanisms to take advantage of these organelles. Most models of *Chlamydia*-host interaction assume that the inclusion membrane prevents direct contact of lumenal bacteria with cytoplasmic contents, and fusion with host membrane bound secretory vesicles and MVBs is the main source for lipid and nutrient uptake (6, 8). Here, we report an unusual mechanism of lipid acquisition by a bacterial pathogen wherein an intact lipid-rich organelle is translocated into the parasitophorous vacuole.

Despite the apparent vectorial transport of LDs into the inclusion lumen, we did not observe a net accumulation of these organelles, suggesting that LDs are consumed after translocation. Consistent with this, the PL monolayers of LDs are highly enriched for phosphatidylcholine (PC) and lyso-PC (28). These PLs are not synthesized by *Chlamydia* but constitute ≈40% of the chlamydial PL content (4). Given that intrainclusion LDs make extensive contacts with RBs (Fig. 2 *D* and *E* and Fig. 3*A*), we speculate that PC and lyso-PC may be acquired directly from LDs by direct membrane contact as has been suggested for ER, mitochondria and Golgi membranes (29). A more efficient use of LDs as a lipid source would require the degradation of neutral lipids. The mechanism of lipolysis is unclear, because *Chlamydia* does not encode proteins with homology to known triacylglycerol (TAG) lipases. However, the *C. trachomatis* genome is predicted to encode one putative lysophospholipase and six phospholipase D (PLD)-like lipases (30). Although these PLDs have been postulated to hydrolyze PC, their substrate specificity *in vivo* is unknown (31). An alternative means of processing

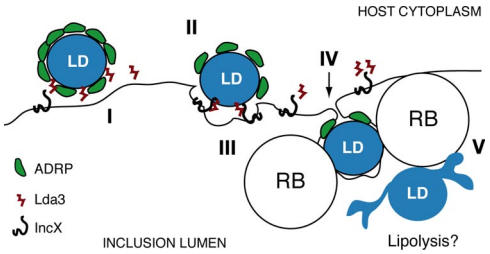

Fig. 5. A model for LD interaction with the *Chlamydia* inclusion. (I) LDs are engaged by secreted Lda3 at the surface of the inclusion. (II) Lda3-tagged LDs are captured at the inclusion membrane by an unidentified inclusion membrane protein(s) (IncX). (III) The inclusion membrane invaginates to deliver the LD to the inclusion lumen. (IV) RBs intimately bind to the intrainclusion LD and associated inclusion membranes. Lda3 may participate in initiating LD lipolysis by promoting the removal of ADRP.

neutral lipids in LDs may be provided by the organelle itself, which comes prepacked with TAG lipases like ATGL, whose activity is normally repressed by ADRP (15). Similarly, MVB-mediated protein traffic could deliver endosomal neutral lipid lipases to the inclusion (32). Regardless of the source, lipase activity is likely essential for chlamydial replication, because treatment of infected cells with the lipase inhibitor E-600 (33) severely impaired inclusion expansion (data not shown). The catabolism of neutral lipids generates fatty acids and glycerol, which can be used for energy generation or as precursors for membrane lipid biosynthesis. However, because *Chlamydiae* lack the enzymes required for β-oxidation of fatty acids, we favor a model wherein LCFA chains released from neutral lipids are used for membrane biosynthesis. Consistent with this, the acyl chains of LD TAGs consist mostly of 18:1, 18:0, and 16:0 fatty acids (28), a composition similar to that of *C. trachomatis* PLs (4).

Although the molecular basis for the capture and translocation of LDs into the inclusion lumen remains to be elucidated, our findings suggest a potential role for the bacterial protein Lda3. Lda3 is a 12-kDa (104-aa) polypeptide that is secreted into the host cytoplasm and accumulates at the inclusion periphery (12). When ectopically expressed, Lda3 has tropism for both LDs and the inclusion membrane indicating its potential to act as molecular bridge between them. Overexpression of Lda3 also leads to the redistribution and loss of ADRP from the surface of LDs (Fig. 4). Furthermore, Lda3 interacts with itself by yeast two-hybrid analysis (data not shown), suggesting that it can form dimers if not higher order structures that may aid in the clustering of proteins required for LD translocation. Based on our live cell observations and TEM analysis, we propose a model for events during LD capture and translocation into the inclusion lumen (Fig. 5). Secreted Lda3 binds to LDs in the vicinity of the inclusion. The Lda3-tagged LDs then dock with the inclusion membrane by binding to a hypothetical chlamydial protein (IncX). Last, the inclusion membrane invaginates to deliver an intact LD into the inclusion lumen, where it is engaged by RBs. Lda3 may also participate in this process by aiding in the localized displacement of ADRP from the LD surface, presumably to promote lipolysis. Although Lda3 has properties compatible with a role in LD entry, limitations of the experimental system preclude us from excluding additional factors or conducting direct tests by mutational analysis. Interestingly, the membranes associated with intralumenal LDs appear to be distinct from the bulk of inclusion membranes as IncA was the only Inc tested that cofractionated with LDs (Fig. 3*C*) and accumulated in the inclusion lumen (Fig. 3*D*). These findings suggest that IncA may mark inclusion membrane sites permissive for LD entry, although we have no evidence that IncA is required for this process.

In summary, we have found that cytoplasmic LDs are translocated into the lumen of the *Chlamydia trachomatis* inclusion, providing an alternative to Golgi-derived vesicles and MVBs for lipid acquisition. This pathogenic strategy would allow *Chlamydia* to remain hidden from innate immune surveillance in the cytoplasm while directly obtaining nutrients. Furthermore, by sequestering lipolysis in the inclusion lumen, the bacteria can limit the release of toxic byproducts that activate inflammatory responses. Whether organelle translocation into the inclusion is restricted to LDs or it represents a more generalized strategy for nutrient acquisition remains to be determined.

Materials and Methods

Strains, Infections, and Cell Culture Reagents. HeLa cells were obtained from ATCC and passaged in DMEM supplemented with 10% Fetal Bovine Serum (Invitrogen). *C. trachomatis* LGV-L2 was propagated and stored as EBs in SPG (0.25 M sucrose, 10 mM sodium phosphate, and 5 mM L-glutamic acid) as described in ref. 34. *C. trachomatis* serovar C and MoPn EBs were obtained from H. Caldwell (Rocky Mountain Laboratories, National Institutes of Health). For infections, EBs were diluted in DMEM, added to HeLa monolayers at an MOI of 0.5–1 and centrifuged at 1,600 $\times$ *g* for 30 min at 4°C. Cells were incubated at 37°C/5% CO_2 for 30 min. Then, cells were washed with PBS, media was replaced, and plates were returned to 5% CO_2 at 37°C for the indicated times. For lipid loading experiments, oleic acid (Sigma) was precomplexed with fatty acid-free BSA (Sigma) in PBS and emulsified by sonication. Oleic acid was added to growth media at final concentration of 100 μM.

Expression Constructs and Antibodies. HeLa cells stably expressing EGFP-ADRP were obtained from P. Targett-Adams and J. McLauchlan (Medical Research Council Virology Unit, Institute of Virology, Glasgow, U.K.) and were derived as described in ref. 35. Lda3-EGFP and Lda3-DsRed were generated by inserting Lda3 (CT473) coding sequence (30) into pEGFP-N1 and pDsRed-N1 (Clontech). Transfections were performed with FuGene6 reagent (Roche) as detailed by the manufacturer. Antibodies were from the following sources: ADRP (ProGen Biotechnik), Nsdhl (M. Ohashi, Okasaki Institute, Okasaki, Japan), Rab1 and 14–3-3β (Santa Cruz Biotechnology), Rab11 (BD Biosciences), Omp2 (RDI) and Cap1 (M. Starnbach, Harvard Medical School, Boston, MA). Mouse monoclonal anti-IncA and anti-CT223 antibodies were obtained from D. Rockey (Oregon State University, Corvallis, OR). Anti-IncG antibodies have been described (36). Polyclonal antibodies to IncA and CT229 were generated by immunizing rabbits with purified GST-IncA (80–324 aa) and GST-CT229 (92–215 aa), respectively.

Fluorescence Microscopy. For indirect immunofluorescence, infected cells were fixed in 3% formaldehyde and 0.025% glutaraldehyde in PBS for 20 min at room temperature. Cells were permeabilized and blocked in 0.05% saponin and 0.2% BSA/PBS (SBP) then incubated with primary antibodies to LD and bacterial proteins, followed by Alexa Fluor-conjugated anti-mouse or anti-rabbit IgG secondary antibodies (Invitrogen). For assessing intrainclusion accumulation of IncA and IncG, fixed cells were permeabilized in 0.1% Triton X-100 for 10 min and blocked in 5% BSA/PBS. For neutral lipid stains, fixed cells were incubated with a 1:1,000 dilution of a saturated acetone solution of BODIPY 493/503 (Invitrogen) in PBS. Nuclei and bacterial DNA were stained with Topro3 (Invitrogen). Fluorescence images were acquired with a Leica TCS Scanning Laser Confocal Microscope. *P* values shown in Figs. 3*D* and 4*F* were determined by one-way ANOVA Tukey–Kramer multiple comparisons test.

Live Cell Microscopy. See *SI Materials and Methods* for experimental details.

Transmission Electron Microscopy. Samples were fixed for 2 h at room temperature with 2.5% glutaraldehyde and 0.05% malachite green (EMS) in 0.1 M sodium cacodylate buffer, pH 6.8. Samples were post-fixed for 30 min with 0.5% osmium tetroxide and 0.8% potassium ferricyanide in 0.1 M sodium cacodylate, for 1 h in 1% tannic acid, and for 1 h in 1% uranyl acetate at room temperature. Specimens were dehydrated with a graded ethanol series, and embedded in Spurr's resin. Thin sections were cut with an RMC MT-7000 ultramicrotome (Ventana) stained with 1% uranyl acetate and Reynold's lead citrate before viewing at 80 kV on a Philips CM-10 transmission electron microscope (FEI). Digital images were acquired with an AMT digital camera system (AMT).

LD Analysis. LDs were isolated from HeLa cells as described in ref. 37. Briefly, two T-175 flasks were either infected with LGV L2 (MOI$\approx$5) or left uninfected.

Gentamicin (100 μg/ml) and oleic acid (100 μM) were added to cells 12–14 h before harvesting LDs at the end of the infectious cycle (40 h). Cells were washed with PBS and harvested in 5 ml of TNE [20 mM Tris·Cl (pH 8.0), 120 mM NaCl, and 2 mM EDTA] containing protease inhibitors (Roche Diagnostics). The cells were lysed on ice with $\approx$40 strokes in a Dounce homogenizer, cell lysates were adjusted to 0.45 M sucrose; overlaid with 2 ml of each of 0.25 M, 0.15 M, and 0 M Sucrose/TNE; and centrifuged at 30,000 rpm for 90 min in an SW41 rotor (Beckman Coulter). The floating LD-enriched fat cake was collected, diluted in TNE, and refloated at 47,000 rpm for 45 min in a TLA55 rotor (Beckman Coulter). LDs were collected, and lipids were extracted with 4 vol of diethyl ether. De-lipidated proteins were precipitated with ice-cold acetone, solubilized in 0.1%SDS and 0.1N NaOH, and normalized for total protein content before SDS/PAGE and immunoblot analysis.

ACKNOWLEDGMENTS. We thank J. McLauchlan for EGFP-ADRP expression cell lines; M. Ohashi, H. Caldwell, M. Starnbach, and D. Rockey for antibodies and strains; C. Jackson (National Institute of Child Health and Human Development, National Institute of Health, Bethesda, MD) for ATGL expression plasmids; Anton Xavier for technical assistance; and Alex Saka for help with statistical analysis. This work was supported by the Whitehead Foundation, the Pew Scholars Program in Biomedical Sciences, National Institutes of Health Grant AI068032 (to R.H.V.), and a Predoctoral Fellowship from the American Heart Association (to J.L.C.).

1. Schachter J (1999) in *Chlamydia: Intracellular Biology, Pathogenesis, and Immunity*, ed Stephens RS (ASM, Washington, D.C.), pp 139–169.
2. Belland R, Ojcius DM, Byrne GI (2004) *Chlamydia. Nat Rev Microbiol* 2:530–531.
3. Fields KA, Hackstadt T (2002) The chlamydial inclusion: Escape from the endocytic pathway. *Annu Rev Cell Dev Biol* 18:221–245.
4. Wylie JL, Hatch GM, McClarty G (1997) Host cell phospholipids are trafficked to and then modified by *Chlamydia trachomatis. J Bacteriol* 179:7233–7242.
5. Hackstadt T, Scidmore MA, Rockey DD (1995) Lipid metabolism in *Chlamydia trachomatis*-infected cells: Directed trafficking of Golgi-derived sphingolipids to the chlamydial inclusion. *Proc Natl Acad Sci USA* 92:4877–4881.
6. Carabeo RA, Mead DJ, Hackstadt T (2003) Golgi-dependent transport of cholesterol to the *Chlamydia trachomatis* inclusion. *Proc Natl Acad Sci USA* 100:6771–6776.
7. Hackstadt T, Rockey DD, Heinzen RA, Scidmore MA (1996) Chlamydia trachomatis interrupts an exocytic pathway to acquire endogenously synthesized sphingomyelin in transit from the Golgi apparatus to the plasma membrane. *EMBO J* 15:964–977.
8. Beatty WL (2006) Trafficking from CD63-positive late endocytic multivesicular bodies is essential for intracellular development of *Chlamydia trachomatis. J Cell Sci* 119:350–359.
9. Su H, *et al.* (2004) Activation of Raf/MEK/ERK/cPLA2 signaling pathway is essential for chlamydial acquisition of host glycerophospholipids. *J Biol Chem* 279:9409–9416.
10. Heinzen RA, Hackstadt T (1997) The *Chlamydia trachomatis* parasitophorous vacuolar membrane is not passively permeable to low-molecular-weight compounds. *Infect Immun* 65:1088–1094.
11. Rockey DD, Scidmore MA, Bannantine JP, Brown WJ (2002) Proteins in the chlamydial inclusion membrane. *Microbes Infect* 4:333–340.
12. Kumar Y, Cocchiaro J, Valdivia RH (2006) The obligate intracellular pathogen *Chlamydia trachomatis* targets host lipid droplets. *Curr Biol* 16:1646–1651.
13. Martin S, Parton RG (2006) Lipid droplets: A unified view of a dynamic organelle. *Nat Rev Mol Cell Biol* 7:373–378.
14. Brasaemle DL (2007) Thematic review series: Adipocyte biology. The perilipin family of structural lipid droplet proteins: Stabilization of lipid droplets and control of lipolysis. *J Lipid Res* 48:2547–2559.
15. Listenberger LL, Ostermeyer-Fay AG, Goldberg EB, Brown WJ, Brown DA (2007) Adipocyte differentiation-related protein reduces the lipid droplet association of adipose triglyceride lipase and slows triacylglycerol turnover. *J Lipid Res* 48:2751–2761.
16. Murphy DJ (2001) The biogenesis and functions of lipid bodies in animals, plants and microorganisms. *Prog Lipid Res* 40:325–438.
17. Liu P, *et al.* (2007) Rab-regulated interaction of early endosomes with lipid droplets. *Biochim Biophys Acta* 1773:784–793.
18. Liu P, *et al.* (2004) Chinese hamster ovary K2 cell lipid droplets appear to be metabolic organelles involved in membrane traffic. *J Biol Chem* 279:3787–3792.
19. Bozza PT, Melo RC, Bandeira-Melo C (2007) Leukocyte lipid bodies regulation and function: Contribution to allergy and host defense. *Pharmacol Ther* 113:30–49.
20. Teichman RJ, Fujimoto M, Yanagimachi R (1972) A previously unrecognized material in mammalian spermatozoa as revealed by malachite green and pyronine. *Biol Reprod* 7:73–81.
21. Scidmore MA, Hackstadt T (2001) Mammalian 14–3-3beta associates with the *Chlamydia trachomatis* inclusion membrane via its interaction with IncG. *Mol Microbiol* 39:1638–1650.
22. Rzomp KA, Scholtes LD, Briggs BJ, Whittaker GR, Scidmore MA (2003) Rab GTPases are recruited to chlamydial inclusions in both a species-dependent and species-independent manner. *Infect Immun* 71:5855–5870.
23. Rockey DD, *et al.* (1997) *Chlamydia psittaci* IncA is phosphorylated by the host cell and is exposed on the cytoplasmic face of the developing inclusion. *Mol Microbiol* 24:217–228.
24. Welte MA (2007) Proteins under new management: Lipid droplets deliver. *Trends Cell Biol* 17:363–369.
25. Smirnova E, *et al.* (2006) ATGL has a key role in lipid droplet/adiposome degradation in mammalian cells. *EMBO Rep* 7:106–113.
26. Hatch GM, McClarty G (1998) Cardiolipin remodeling in eukaryotic cells infected with *Chlamydia trachomatis* is linked to elevated mitochondrial metabolism. *Biochem Biophys Res Commun* 243:356–360.
27. Wang G, Burczynski F, Anderson J, Zhong G (2007) Effect of host fatty acid-binding protein and fatty acid uptake on growth of *Chlamydia trachomatis* L2. *Microbiology* 153:1935–1939.
28. Bartz R, *et al.* (2007) Lipidomics reveals that adiposomes store ether lipids and mediate phospholipid traffic. *J Lipid Res* 48:837–847.
29. Holthuis JC, Levine TP (2005) Lipid traffic: Floppy drives and a superhighway. *Nat Rev Mol Cell Biol* 6:209–220.
30. Stephens RS, *et al.* (1998) Genome sequence of an obligate intracellular pathogen of humans: *Chlamydia trachomatis. Science* 282:754–759.
31. Nelson DE, *et al.* (2006) Inhibition of chlamydiae by primary alcohols correlates with the strain-specific complement of plasticity zone phospholipase D genes. *Infect Immun* 74:73–80.
32. Fu D, Hornick CA (1995) Modulation of lipid metabolism at rat hepatic subcellular sites by female sex hormones. *Biochim Biophys Acta* 1254:267–273.
33. Gilham D, *et al.* (2003) Inhibitors of hepatic microsomal triacylglycerol hydrolase decrease very low density lipoprotein secretion. *FASEB J* 17:1685–1687.
34. Caldwell HD, Kromhout J, Schachter J (1981) Purification and partial characterization of the major outer membrane protein of *Chlamydia trachomatis. Infect Immun* 31:1161–1176.
35. Targett-Adams P, *et al.* (2003) Live cell analysis and targeting of the lipid droplet-binding adipocyte differentiation-related protein. *J Biol Chem* 278:15998–16007.
36. Scidmore-Carlson MA, Shaw EI, Dooley CA, Fischer ER, Hackstadt T (1999) Identification and characterization of a *Chlamydia trachomatis* early operon encoding four novel inclusion membrane proteins. *Mol Microbiol* 33:753–765.
37. Umlauf E, *et al.* (2004) Association of stomatin with lipid bodies. *J Biol Chem* 279:23699–23709.